

fore, *S. cardiophyllum* must be assigned an EBN of 1. This demonstrates that effective ploidy (EBN) differences can function as a barrier to hybridization between diploid species.

Crosses 5 and 6 (Table 1) indicate that the non-tuber-bearing species *S. fernandezianum* can also be assigned an EBN of 1 (12). Crosses 7, 8, and 9 demonstrate that *S. commersonii* is also 1EBN. This is especially remarkable because *S. commersonii* is sympatric and considered closely related to 2x (2EBN) *S. chacoense* (6).

To demonstrate the potential usefulness of the EBN concept we applied the knowledge of the EBN assignments stated above to create a new hybrid. Diploid ( $2n = 2x = 24$ ) *S. brevidens* is a non-tuber-bearing species of Series Etuberosa which crosses readily with *S. fernandezianum*; therefore, it should also be 1EBN. In crosses of 2x (1EBN) *S. brevidens* × 2x (2EBN) *S. chacoense*, the hybrid seeds were abortive and the embryos could not be rescued by embryo culture (cross 10, Table 1). However, when colchicine-induced 4x (2EBN) *S. brevidens* was crossed with 2x (2EBN) *S. chacoense* the seeds were much better developed (cross 11, Table 1). Without special treatment, one hybrid seed germinated, producing a vigorous plant that was clearly hybrid (12) (Fig. 1). Since the hybrid seeds did not have completely normal endosperm development in the 4x (2EBN) *S. brevidens* × 2x (2EBN) *S. chacoense* cross, either the EBN assigned *S. brevidens* is not precisely 1 or there are other factors involved in endosperm development. Employing a meiotic mutant of 2x (1EBN) *S. commersonii*, which produces 2n pollen and therefore delivers 2EBN to the egg and central cell, we have also produced hybrids between 2x (1EBN) *S. commersonii* and 2x (2EBN) *S. chacoense*.

We have demonstrated that effective ploidy (EBN) barriers exist between diploid *Solanum* species and that, with knowledge of EBN's, ploidies can be manipulated (13) to produce new and potentially useful hybrids. Since the EBN concept is probably applicable to many other angiosperm genera (2), it could be employed to break crossing barriers between other crops and their wild relatives.

S. A. JOHNSTON\*

Department of Horticulture,  
University of Wisconsin,  
Madison 53706

R. E. HANNEMAN, JR.  
Agricultural Research Service and  
Department of Horticulture,  
University of Wisconsin

#### References and Notes

1. R. A. Brink and D. C. Cooper, *Bot. Rev.* **13**, 423 (1947).
2. S. A. Johnston, T. P. M. den Nijs, S. J. Peloquin, R. E. Hanneman, Jr., *Theor. Appl. Genet.* **57**, 5 (1980); S. A. Johnston, thesis, University of Wisconsin, Madison (1980). The EBN concept is similar to an idea reported by I. Nishiyama and T. Yabuno [*Cytologia* **43**, 453 (1978)].
3. B. Y. Lin, thesis, University of Wisconsin Madison (1975).
4. Y. Irikura, *Res. Bull. Hokkaido Natl. Agric. Exp. Stn.* **92**, 23 (1968).
5. S. A. Johnston and R. E. Hanneman, Jr., *Am. Potato J.* **57**, 7 (1980).
6. J. G. Hawkes, in *The Biology and Taxonomy of the Solanaceae*, J. G. Hawkes, R. N. Lester, A. D. Skelding, Eds. (Academic Press, London, 1979), pp. 637-646.
7. J. S. Neiderhauser and W. R. Mills, *Phytopathology* **43**, 456 (1953).
8. K. K. Pandey, *Am. J. Bot.* **49**, 874 (1962); R. W. Hougas and S. J. Peloquin, *Eur. Potato J.* **3**, 325 (1960); J. G. Hermsen and M. S. Ramanna, *Euphytica* **25**, 1 (1976).
9. R. W. Ross and P. R. Rowe, *Am. Potato J.* **46**, 5 (1969).
10. R. A. C. Jones, *Potato Res.* **22**, 149 (1979).
11. J. G. Hermsen and L. M. Taylor, *Euphytica* **28**, 1 (1979).
12. Two of the interspecific crosses were between tuber-bearing and non-tuber-bearing species: 2x *S. fernandezianum* × 2x *S. cardiophyllum* and 4x *S. brevidens* × 2x *S. chacoense*. The  $F_1$ 's showed hybrid vigor and flowered. Neither type of hybrid could be induced to produce tubers under a variety of temperature and light regimes. However, both types of  $F_1$ 's produced stolons, which neither *S. fernandezianum* nor *S. brevidens* do.
13. In the experiments described the maternal:paternal EBN ratios in the endosperm were changed by altering the numerical ploidy of one of the parents. However, conceivably the EBN could be changed by altering the dose or character of one chromosome or one gene. We have evidence from experiments in *Datura stramonium* that, at most, two of its 12 chromosomes determine the EBN.
14. This work is a cooperative investigation of the Agricultural Research Service, U.S. Department of Agriculture, and the Wisconsin Agricultural Experiment Station.

\* Present address: Department of Biological Chemistry, M. S. Hershey Medical Center, Hershey, Pa. 17033.

23 November 1981; revised 5 April 1982

## Changes in the Cell Membranes of the Bullfrog Gastric Mucosa with Acid Secretion

**Abstract.** *The effective area, resistance, and configuration of the apical and basolateral cell membranes of the bullfrog gastric mucosa were studied as a function of acid secretion rate, by alternating-current impedance methods. The drop in transepithelial resistance with acid secretion is attributed to the great increase in apical membrane area (hence conductance) associated with tubulovesicles. There is no evidence of a change in basolateral membrane resistance or of apical membrane permeability per unit area.*

Acid secretion by the gastric mucosa is one of the more spectacular, complex, and less well understood epithelial transport systems. The large morphological and electrical changes that accompany acid secretion provide clues to its mechanism. With the onset of secretion, there is an enormous increase of apical membrane area due probably (1) to the fusion of intracellular vesicles and tubules into the apical membrane (so-called "tubulovesicles") (2, 3), and a drop in the transepithelial resistance ( $R_t$ ) (4). Even in the resting mucosa,  $R_t$  has the surprisingly low value of a few hundred ohm-cm<sup>2</sup>, a value in the range of epithelia with leaky junctions, although in other respects the stomach resembles a tight epithelium (5). This low  $R_t$  (high transepithelial conductance) is especially surprising in view of the low permeability of the undamaged stomach to  $H^+$  (the so-called mucosal permeability barrier, whose breakdown is associated with peptic ulcers).

Could this high conductance be due to large membrane area? Because of tissue folding and cell surface elaborations such as microvilli, the true membrane area of an epithelium exceeds its nominal flat area, often by a large factor. This multiplication of area would tend to yield

a low  $R_t$  value normalized to nominal area.

A potentially relevant experimental technique is equivalent electrical circuit analysis by impedance methods, which can yield the apical and basolateral membrane resistances ( $R_a$  and  $R_b$ ) and capacitances ( $C_a$  and  $C_b$ ) of the epithelial cells. Capacitance values are useful as an estimate of the true membrane area, since the capacitances of biological membranes cluster around 1  $\mu F$  cm<sup>-2</sup> (6). In addition, infolded structures such as lateral intercellular spaces (LIS) and tubulovesicles behave as distributed resistors (7) whose electrical properties depend on their ratio of cross-sectional area to length, so that impedance analysis can yield information about ultrastructural geometry nondestructively in an unfixed preparation. We have developed methods for alternating-current (a-c) impedance analysis of a tight epithelium, the rabbit urinary bladder, and found that the analysis yielded values of  $R_a$ ,  $R_b$ ,  $C_a$ ,  $C_b$ , and the area/length ratio of the LIS in agreement with independent measures (8). By extending this approach to the gastric mucosa, we hoped (i) to monitor (as  $C_a$  and  $C_b$ ) the changes in apical and basolateral membrane areas with HCl secretion, (ii) to establish whether the

apparently low value of  $R_i$  just reflects the increase of membrane area due to gastric crypts, microvilli, and tubulovesicles, and (iii) to examine whether the decrease in  $R_i$  with secretion is due to the associated increase in apical membrane area (reflected in increased  $C_a$ ), or whether it implies in addition a membrane permeability change (reflected in decreased  $R_a$  normalized to  $C_a$ ) or a change in basolateral membrane properties.

A 2-cm<sup>2</sup> piece of bullfrog gastric mucosa from the fundic region of the stomach was stripped of its underlying musculature and mounted between chambers, each with a volume of 15 ml. The chamber design virtually eliminated edge damage (9). The serosal (nutrient) solution had the composition 86 mM NaCl, 5 mM KCl, 1 mM MgCl<sub>2</sub>, 18 mM NaHCO<sub>3</sub>, 1 mM NaH<sub>2</sub>PO<sub>4</sub>, and 10 mM D-glucose at pH 7.3. The mucosal (secretory) solution was nominally buffer-free 120 mM NaCl maintained at pH 5.0 by a pH-stat. Both solutions were gassed with a mixture of 95 percent O<sub>2</sub> and 5 percent CO<sub>2</sub> and stirred with magnetic fleas. The HCl secretion was stimulated by 10<sup>-4</sup>M histamine or inhibited by 10<sup>-4</sup>M cimetidine, and its rate was measured continuously by the pH-stat.

For a-c impedance analysis we used 25 frequencies of sinusoidal constant current in the range of 1 Hz to 10 kHz (10). The tissue's voltage response was measured with a dual-phase phase lock amplifier. Impedance measurements were corrected for small phase errors of the preamplifier and chamber and for the slight frequency dependence of preamplifier gain. Data were represented as Bode plots, plots of phase angle and the logarithm of the magnitude versus the logarithm of the frequency [see (8) for a discussion of the advantages of this representation in epithelial impedance studies]. A set of experimental measurements took 12 minutes and was made during a period when the acid secretion rate was at steady state.

The following equivalent circuit models were used to fit the data (Fig. 1). (i) In the simplest model, the lumped one-cell model, the apical and basolateral membranes of the epithelial cells are represented as discrete (lumped) parallel RC circuit elements. In series with the two cell membranes is a series resistance ( $R_s$ ) arising from the adjacent unstirred layers, connective tissues, and muscle. As the gastric mucosa has several cell types, in this model it is assumed that there is good lateral coupling among cells and each RC element represents the mean properties of different cell types. Junctional

conductance is assumed negligible in this model as well as in the other two models (11). (ii) The lumped two-cell model differs in that the two major cell types, the oxyntic cells and surface epithelial cells, are considered electrically isolated from each other, and each has its own values of  $R_a$ ,  $C_a$ ,  $R_b$ , and  $C_b$  (differentiated by superscripts, such as  $R_a$  and  $R'_a$ , for the two cell types). Although this model has nine circuit elements, four more than the lumped one-cell model, it reduces to a seven-element circuit in which each element is now a complicated function of the original elements and no longer has a simple morphological counterpart. (iii) The distributed model is a one-cell model differing from the lumped one-cell model in that both the basolateral and apical membranes are represented as distributed impedances. We model the long and narrow LIS at the basolateral membrane and the gastric crypts at the apical surface as distributed resistors. This model also has seven parameters (12).

The results of 16 sets of impedance measurements were fitted to each of these three models, and the best-fit circuit parameters were calculated by the methods described in (8, 13, 14). These experiments gave six main results:

1) The impedance data yield two time constants ( $\tau = RC$ ) differing by about an order of magnitude (about 2 and 20 msec). The slow  $\tau$  has a higher capacitance than the fast  $\tau$ . The capacitance values of the slow  $\tau$  and fast  $\tau$  increase, respectively, by factors of up to 100 and less than 2 with increasing HCl secretion rate. We conclude that the slow and fast  $\tau$  values correspond, respectively, to the apical and basolateral membranes, because electron microscopy shows that the apical membrane area exceeds the basolateral membrane area (2) and increases at least tenfold with HCl secretion (2, 15), while the basolateral membrane area changes little with HCl secretion [see (12), sentence 3].

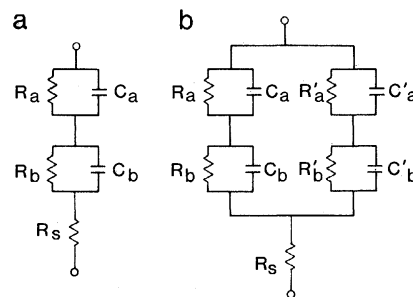
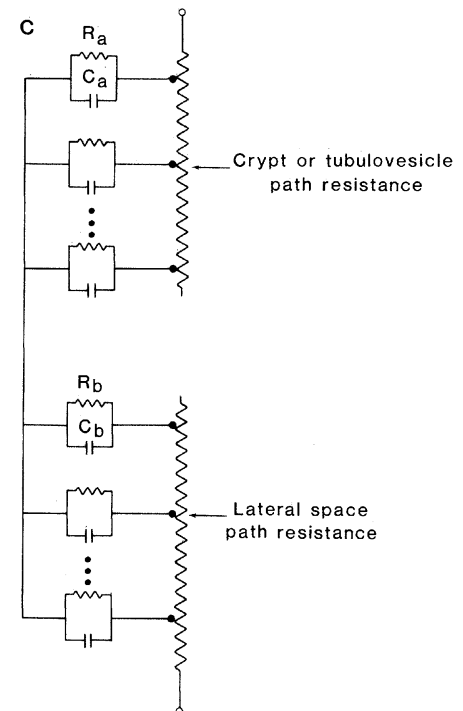


Fig. 1. Three alternative equivalent-circuit models for the gastric mucosa (see text): (a) lumped one-cell model, (b) lumped two-cell model, and (c) distributed model.

2) The lumped one-cell and two-cell models give systematic misfits to the impedance data, which are eliminated if the distributed model is used, though it has no more parameters than the lumped two-cell model (Fig. 2). A modified *F*-test shows that the two additional parameters that the distributed model possesses over the lumped one-cell model are highly significant ( $P \ll 10^{-6}$ ). The lumped models yield not only systematic misfits but also unreasonable values of the parameters (8). Our remaining discussion of parameter values refers to those extracted by use of the distributed model (16).

3) The values of  $C_b$  have a mean  $\pm$  the standard error of the mean of  $99 \pm 15 \mu\text{F cm}^{-2}$  ( $N = 16$ ), implying about 100 cm<sup>2</sup> of basolateral membrane area per square centimeter of exposed chamber area [see (10), last sentence]. This value is in good agreement with the value obtained by morphometric analysis of the oxyntic cells alone, 89 cm<sup>2</sup> per square centimeter of exposed chamber area (2). The origin of this large amplification of membrane area is threefold: (i) apical and basolateral membrane areas must exceed chamber area because the whole epithelium has infoldings, the gastric crypts; (ii) a smooth cuboidal cell would have five times as much basolateral area as apical area; (iii) the basolateral cell membranes themselves are extensively folded. The extracted  $C_b$  is relatively independent of HCl secretion rate, in agreement with morphological findings that the basolateral membrane



does not change with acid secretion.

4) Related to chamber area,  $R_b$  is  $41 \pm 5$  ohm-cm<sup>2</sup>, which would be an absurdly low value for a flat epithelium without infolding (for example, frog skin and rabbit urinary bladder). However, when normalized to  $C_b$  as a measure of real basolateral membrane area, one obtains  $3.5 \pm 0.6$  kilohm- $\mu$ F (that is, about 3.5 kilohm for  $\sim 1$ -cm<sup>2</sup> real area). This value is similar to that for frog skin and rabbit urinary bladder (17). The mean  $R_t$  related to chamber area is 89 ohm-cm<sup>2</sup>, far lower than for almost any other tight epithelium. This value becomes 8.8 kilohm- $\mu$ F ( $\sim 8.8$  kilohm for 1-cm<sup>2</sup> real area) when normalized to basolateral membrane area, a typical value for a flat, tight epithelium. Thus, the apparently low  $R_t$  of the stomach is misleading, because 1 cm<sup>2</sup> of chamber area corresponds to 100 cm<sup>2</sup> of basolateral membrane area. The  $R_b$  is independent of acid secretion rate.

5) The value of  $C_a$  increases dramatically with acid secretion rate, from 200  $\mu$ F cm<sup>-2</sup> at low rates (below 1  $\mu$ eq H<sup>+</sup> cm<sup>-2</sup> hour<sup>-1</sup>) to over 8000  $\mu$ F cm<sup>-2</sup> at high rates (above 4  $\mu$ eq H<sup>+</sup> cm<sup>-2</sup> hour<sup>-1</sup>). In every individual experiment,  $C_a$  increased when acid secretion was stimulated by histamine (four experiments) and decreased when it was inhibited by cimetidine (five experiments). This increase in  $C_a$  with secretion, by 40-fold or more, corresponds to the great increase in membrane area with secretion observed in morphometric studies (2). [Quantitative comparison of the factor is not possible, because in the morphometric studies there was no attempt to quantify the area of the tubulovesicles. Morphometric analysis surely underestimates the actual increase in apical membrane area observed during stimulation (2).] The high  $C_a$  value even at low acid secretion rates,  $\sim 200$  cm<sup>2</sup> of apical membrane area per square centimeter of chamber area, reflects in part the infolded gastric crypts, in part the tubulovesicles, many of which are connected to the apical membrane area in the nonsecreting state in the bullfrog stomach (18).

6) The value of  $R_a$  normalized to the chamber area decreases dramatically with acid secretion rate, from 150 ohm-cm<sup>2</sup> at low rates to 4.6 ohm-cm<sup>2</sup> at high rates. But when  $R_a$  is normalized to  $C_a$  as a measure of actual apical membrane area, the resulting mean  $R_a$  value of  $25 \pm 4$  kilohm- $\mu$ F ( $N = 16$ ) is independent of acid secretion rate. Thus, the decrease in  $R_a$  with acid secretion is largely explained in terms of an increase in membrane area: we have no evidence

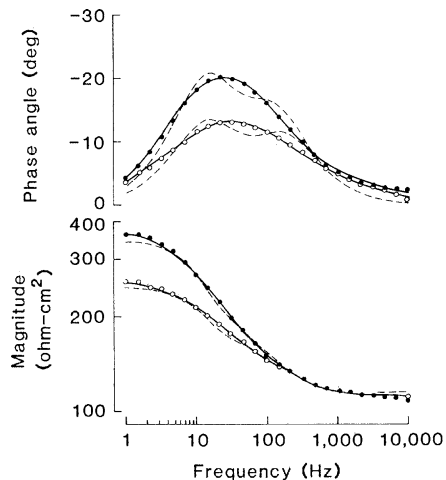


Fig. 2. Comparison of the fits of the lumped one-cell (---) and distributed (—) models to impedance measurements in a gastric mucosa with acid secretion inhibited by cimetidine (●) and then stimulated by histamine (○). The measured values at low (●) and high (○) secretion rates are very different, the lumped one-cell model gives systematic misfits to the data (especially to the phase angle data), and the distributed model gives good fits. The same misfits are seen with the lumped model in all experiments. The lumped two-cell model also gives systematic misfits (not shown), somewhat less marked than those of the lumped one-cell model.

for an actual change in conductance per unit area or in relative ionic permeability coefficients. Related to actual membrane area, the apical membrane has a considerably higher resistance than the basolateral membrane.

CHRIS CLAUSEN

Department of Physiology and  
Biophysics, State University of  
New York, Stony Brook 11794

TERRY E. MACHEN

Department of Physiology and  
Anatomy, University of California,  
Berkeley 94720

JARED M. DIAMOND

Department of Physiology,  
University of California Medical  
Center, Los Angeles 90024

#### References and Notes

1. The mechanism of membrane elaboration in oxyntic cells is debated: T. Berglinth, D. DiBona, S. Ito, G. Sachs, *Am. J. Physiol.* **238**, G165 (1980); J. Forte *et al.*, *ibid.* **241**, G349 (1981); C. Logsdon and T. Machen, *Anat. Rec.* **202**, 73 (1982).
2. H. Helander, S. Sanders, W. Rehm, B. Hirschowitz, in *Gastric Secretion*, G. Sachs, E. Heinz, K. Ullrich, Eds. (Academic Press, New York, 1972), p. 69; C. Logsdon and T. Machen, *Am. J. Physiol.* **241**, G365 (1981).
3. S. Ito and G. Schofield, *J. Cell Biol.* **63**, 364 (1974).
4. T. Forte, T. Machen, J. Forte, *Gastroenterology* **69**, 1208 (1975).
5. E. Frömter and J. Diamond, *Nature (London)* **235**, 9 (1972).
6. H. Davson, *A Textbook of General Physiology* (Little, Brown, Boston, 1964); K. Cole, *Membranes, Ions, and Impulses* (Univ. of California Press, Berkeley, 1972).
7. A distributed resistor is one that must be mod-

eled as a structure with resistance distributed along its length rather than as a discrete resistor.

8. C. Clausen, S. Lewis, J. Diamond, *Biophys. J.* **26**, 291 (1979).
9. S. Lewis and J. Diamond, *J. Membr. Biol.* **28**, 1 (1976).
10. The application of impedance analysis to the gastric mucosa was pioneered by T. Teorell, W. Rehm, and their colleagues, who applied step inputs of current and analyzed the resulting time-dependent voltage response (so-called transient analysis) [T. Teorell and R. Wersall, *Acta Physiol. Scand.* **10**, 243 (1945); T. Teorell, *ibid.* **12**, 235 (1946); D. Noyes and W. Rehm, *Am. J. Physiol.* **219**, 184 (1970); W. Rehm, S. Sanders, M. Tant, F. Hoffman, J. Tarvin, in *Gastric Hydrogen Secretion*, D. Kasbekar, G. Sachs, W. Rehm, Eds. (Dekker, New York, 1976), p. 29; J. Tarvin, H. Helms, J. Pirkle, W. Rehm, *Biophys. J.* **25**, 30a (1979)]. We found that with this method it was impossible to detect distributed resistors in actual gastric mucosae or in simulated model circuits, because this method gives low weighting to the middle and high frequencies where the effects of distributed resistors become detectable (8, p. 300). The technique of a-c impedance analysis is well suited to detecting distributed resistors, as it can weight all frequencies equally. Failure to detect distributed resistors results in gross errors in estimates of other circuit parameters extracted from the lumped models (8, p. 312). For example, the value of  $C_b = 17$   $\mu$ F cm<sup>-2</sup> extracted by the lumped one-cell model is much lower than one expects from cell ultrastructure.
11. A. Blum, B. Hirschowitz, H. Helander, G. Sachs, in *Gastric Secretion*, G. Sachs, E. Heinz, K. Ullrich, Eds. (Academic Press, New York, 1972), p. 165; T. Machen, W. Silen, J. G. Forte, *Am. J. Physiol.* **234**, E228 (1978).
12. The seven parameters are  $R_a$ ,  $R_b$ ,  $C_a$ , and  $C_b$ ; distributed path resistances ( $R_{ap}$  and  $R_{bp}$ ) at the apical and basolateral surfaces, respectively; and series resistance  $R_s$ . The two membrane time constants  $R_a C_a$  and  $R_b C_b$  differ sufficiently for the gastric mucosa, and the transepithelial impedance data are sufficiently abundant and accurate that unique values of all seven parameters can be extracted from these data alone, in contrast to the case for the rabbit urinary bladder (8) or leaky epithelia. However, other information was required to identify which extracted time constant corresponded to which cell membrane. At the apical surface of the oxyntic cells the long and narrow tubules that are open to the luminal solution, and the narrow intracellular spaces between them, similarly constitute distributed resistors. In practice, it is difficult to decide whether the distributed effects observed experimentally for the apical membrane arise from these tubules or from the gastric crypts.
13. We used a nonlinear least-squares algorithm [K. Brown and J. Dennis, *Numer. Math.* **18**, 289 (1973)] that minimizes the error between the theoretical curves and the experimental data by adjusting the parameter values of the theoretical curves. The phase angle and measurements of the logarithm of the magnitude were normalized to their maximal values for more equal weighting of these two plots, and they were fitted simultaneously. A modified  $F$ -test (14) was used to assess whether each added model parameter is significant, that is, whether the improvement of fit that it causes is significantly greater than expected for a purely random variable. In addition, we calculated the standard deviation of each best-fit parameter and the parameter correlation matrix (14) to assess how well the parameters were determined by the available data.
14. W. Hamilton, *Statistics in Physical Science* (Ronald, New York, 1964).
15. K. Carlisle, C. Chew, S. Hersey, *J. Cell Biol.* **76**, 31 (1978).
16. Why does the distributed model, which is a one-cell model, give an excellent fit although the gastric mucosa has several cell types? The main reason, also supported by other evidence, is probably that the oxyntic cells provide the main conductance pathway because they have much more membrane area (due to the greatly folded apical membrane) than the other cell types. Lateral coupling among cell types may also contribute.
17. S. Lewis, D. Eaton, J. Diamond, *J. Membr. Biol.* **28**, 41 (1976).
18. A. Sedar, *J. Cell Biol.* **43**, 179 (1969).
19. Supported by NIH grants GM 14772, AM 17328 (University of California at Los Angeles Center for Ulcer Research and Education), and AM 19520.

27 October 1981; revised 30 March 1982